Strain Calibration of Substrate-Free FBG Sensors at Cryogenic Temperature

Venkataraman Narayanan Venkatesan[1,2], Klaus-Peter Weiss[1], Ram Prakash Bharti[2], Holger Neumann[1], and Rajinikumar Ramalingam[1(✉)]

[1] Institute for Technical Physics (ITEP), Karlsruhe Institute of Technology (KIT), 76344 Eggenstein-Leopoldshafen, Germany
rajini-kumar.ramalingam@kit.edu
[2] Department of Chemical Engineering, Indian Institute of Technology (IIT) Roorkee, Roorkee 247667, India

Abstract. Strain calibration measurements are performed for acrylate coated, substrate-free fiber Bragg grating (FBG) sensors at room temperature of 298 K and cryogenic temperature of 77 K. A 1550 nm Bragg wavelength (λ_B) FBG sensor, with its sensing part not being bonded to any surface, is subjected to axial strain using MTS25 tensile machine available at Cryogenic Material tests Karlsruhe (CryoMaK), KIT. The Bragg wavelength shift ($\Delta\lambda_B$) versus induced strain (ε) is regressed with a linear polynomial function and the strain sensitivity obtained is found to be 0.9 pm/με at both the temperatures, verifying that the FBG strain sensitivity is independent of temperature.

Keywords: Fiber Bragg gratings (FBG) · Cryogenic applications · Strain sensitivity · Strain calibration

1 Introduction

Over the years, Fiber Bragg gratings (FBG) are being widely used as reliable sensors to monitor crucial parameters like temperature, strain, flowrate, concentration, etc., in various applications [1–3]. FBG sensors are a good replacement for most of the conventional sensors due to their miniature size, high sensitivity, multiplexing capabilities and immunity to electrical and magnetic fields [4, 5]. They have also been proven to be good candidates for accurate measurements at cryogenic temperatures [6–8]. As documented in many literatures [9–11], FBG is a short segment in the core of an optical fiber which has a periodic variation of refractive index. These gratings are inscribed into the optical fiber using UV interferometer [11]. Due to the varying refractive index of the FBG, one particular wavelength of the incident light is reflected and the others are transmitted, as depicted in Fig. 1. This reflected wavelength (central wavelength of the reflected band) is called the Bragg wavelength (λ_B) and it satisfies the following condition [12]:

B. Mandler et al. (Eds.): IoT 360° 2015, Part II, LNICST 170, pp. 191–202, 2016.
DOI: 10.1007/978-3-319-47075-7_24

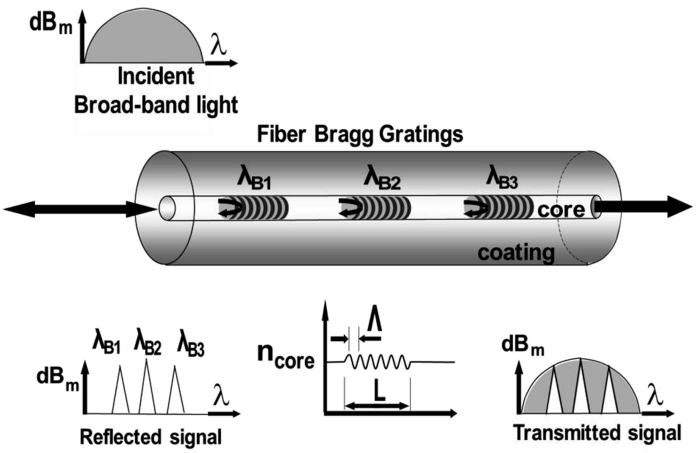

Fig. 1. Principle of fiber Bragg gratings.

$$\lambda_B = 2\Lambda n_{eff} \tag{1}$$

where Λ is the grating period and n_{eff} is the effective refractive index of the FBG.

FBG is sensitive to mechanical strain which causes linear expansion of the gratings, leading to a change in the grating period and refractive index due to photo-elastic effect. The gratings are also sensitive to temperature due to thermal expansion and the thermo-optic effect of the fiber material (usually Germanium doped Silica). Changes in strain (ε) or temperature (ΔT) causes a Bragg wavelength shift ($\Delta\lambda_B$), thus enabling its application in measurement technology. The Bragg wavelength shift can be expressed as [12]:

$$\frac{\Delta\lambda_B}{\lambda_B} = (\alpha_s + \alpha_e)\Delta T + (1 - p_e)\varepsilon \tag{2}$$

where α_s is the thermal expansion coefficient (0.55×10^{-6} for silica), α_e is the thermo-optic coefficient (8.6×10^{-6} for silica) and p_e is the effective strain-optic coefficient of the fiber which can be calculated using [12]:

$$p_e = \frac{n^2}{2}[p_{12} - \nu(p_{11} + p_{12})] \tag{3}$$

where p_{11} and p_{12} are the components of strain-optic tensor, n is the fiber core refractive index, and ν is the Poisson's ratio. For a typical FBG sensor ($p_{11} = 0.113$, $p_{12} = 0.252$, $\nu = 0.16$ and $n = 1.482$), p_e is 0.22. For a Bragg wavelength $\sim$1550 nm, the expected strain sensitivity is 1.2/$\mu\varepsilon$, i.e., for an applied strain of 1 $\mu\varepsilon$, the change in Bragg wavelength will be 1.2 pm. The expected temperature sensitivity is 13.7 pm/K. The strain and temperature sensitivities of the FBG, however, differ from sensor to sensor, thus requiring a calibration of the sensor before using it for any measurement.

Both strain and temperature response of various types of FBG sensors are being investigated and reported regularly. Roths et al. [13] have reported the temperature sensitivity of a bare FBG and an FBG bonded to a poly (methyl methacrylate) substrate, at temperatures ranging from 4.2 K to 300 K. Strain response of FBG sensors at cryogenic temperatures have been reported by James et al. [14] where the FBG sensors were either attached to a stainless steel cantilever or invar sample. The reported strain sensitivities, however, vary depending on a lot of factors like the type of FBG sensor, strain transfer efficiency, gluing techniques used, etc., making it difficult for the comparison of these values. This leads to the importance of studying the strain response without attaching the FBG sensing part to any surface. Such an investigation was carried out by Roths et al. [15] where a 'free' FBG sensor was strained using weights-guided movable clamps attached to the non-sensing part of the fiber. Although this was one of the first reliable methods that can be used for FBG sensor standardization procedures, it was performed only at room temperature.

To the best of our knowledge, strain calibrations of un-bonded or substrate-free FBG sensors at cryogenic temperatures have not been reported so far. This paper discusses the strain response of a substrate-free FBG sensor whose sensing part is not attached to any surface for temperatures of 298 K and 77 K.

2 Experiment

A commercial polyamide coated single mode fiber (SMF 28) containing two FBG sensors is used in this study. Each sensor grating has different spatial period, thus having different Bragg wavelengths, namely, λ_{B1} and λ_{B2}. Of these two FBG sensors, one sensor's (FBG 1) ends are attached firmly to two stainless steel structures, making sure that the FBG sensing part is free and does not have any contact with any surface (Fig. 2). FBG 1 can sense both strain and temperature. The other sensor (FBG 2) is let to hang freely to ensure that there is no strain felt in it and is used to measure only temperature.

The ends of FBG 1 are glued to the metal structures using epoxy-phenol adhesive. This type of glue requires a heat treatment at about 160 °C for 2 h. The heating apparatus (Fig. 3) was supplied by Hochtemperaturöfen GmbH, Germany. The heating tube consists of an uncovered FeCrAl (Iron-Chromium-Aluminium) heating coil which is mounted on a ceramic fiber module. The low thermal conductivity of the ceramic fiber insulation guarantees low energy consumption and allows for high heating rates. The tube is wound with this wire and kept in the center of the furnace to provide

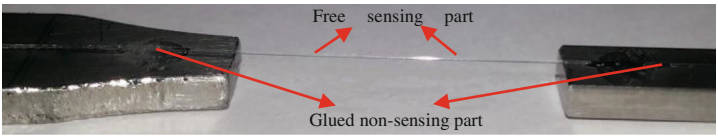

Fig. 2. FBG sensor glued to metal structures with the central sensing part not touching any surface.

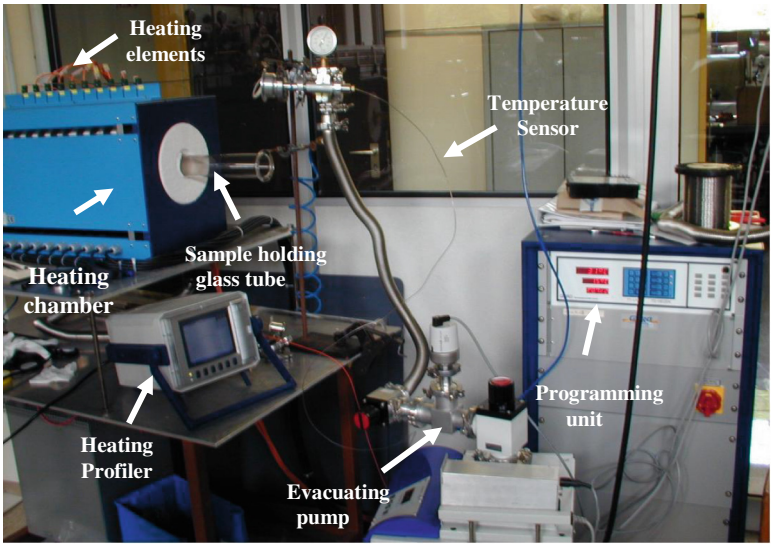

Fig. 3. GERO Hochtemperaturöfen apparatus for heat treatment.

uniform heating. High flexibility in the design of the temperature profile is a special characteristic of this type of furnace. The manual setting of homogenous temperature areas, temperature gradients, maximum temperature limits, heating duration, etc., is possible.

The metal structures with FBG sensors are placed in the glass tube and the maximum heating temperature is set at 160 °C which is well within the maximum limit of temperature the fiber can withstand. The furnace is then started by passing commands in the programming unit with the heating duration set to 2 h.

Once the temperature reaches 160 °C, it stays constant for 2 h and then the furnace gets turned off automatically. The heated sample is allowed to cool naturally till it reaches the room temperature. The spectra of FBG 1 before and after the heat treatment is plotted in Fig. 4. It can be seen that the spectral pattern is almost the same and there is no significant change in the initial Bragg wavelength. Thus, the chosen heat treatment has not affected the FBG sensor properties.

The sample is then transferred to the MTS25 tensile machine with cryostat available at Cryogenic Material tests Karlsruhe (CryoMaK) [16], ITeP, KIT. The tensile machine consists of an extensometer (also called top load cell) and a bottom load cell. An extensometer is a device that is used to measure the distance between two distinct points on the surface of the attached specimen [17, 18]. It is fixed on a Copper-Beryllium (CuBe) wire to measure the applied strain. Figure 5 shows a schematic of an extensometer and the connections that are required to measure the strain felt by the specimen. When there is any strain applied to the specimen (FBG with metal structures in this case), the extensometer attached with the specimen also gets strained. The resistance of the strain gauge glued in the arms of the extensometer vary according to the strain applied on the specimen. The change in the resistance is read out as a

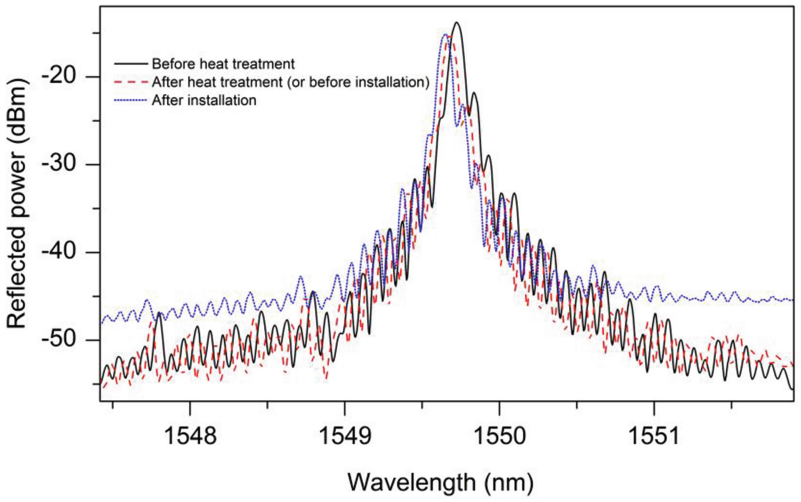

Fig. 4. Spectral comparison of FBG before heat treatment, after heat treatment (same for pre-installation) and after installation.

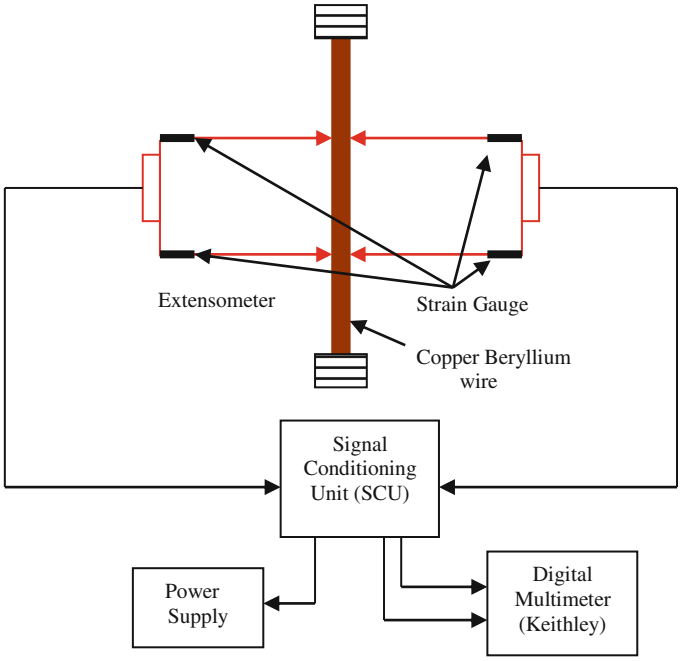

Fig. 5. Schematic of extensometer and its connections.

Table 1. FBG sensor and Braggmeter specifications

FBG Parameter	Specification
Manufacturer	FBGS technologies
Type	DTG®-LBL-1550-F
Diameter (coated)	195 μm
Braggmeter	FS22 Industrial (SI)
Resolution	1.0 pm
Absolute accuracy	±2.0 pm
Repeatability	±1.0 pm
Optical output power	10 dBm
Dynamic range	>50 dB
Optical detection	Logarithmic

millivolt (mV) change for applied strain. Such a contact type extensometer is calibrated by applying known strain and recording the output. The calibrated extensometer is used as a reference sensor for FBG strain calibration. Table 1 lists the parameters of the FBG sensor and Braggmeter considered with their respective specifications. The Braggmeter (FS22 Industrial BraggMETER SI) [19] has a very good resolution of 1.0 pm and absolute accuracy of ±2.0 pm. In other words, temperature can be measured with an accuracy of 0.2 K and strain with 1.7 με. The Braggmeter also has good repeatability of ±1.0 pm, showing that the error in measurement due to the measuring device is negligible.

The metal structures holding the fiber are installed by attaching to the load cells (Fig. 6) of the tensile machine, which has an accuracy of ±1 μm displacement. A pre-strain is given to the sensor to avoid errors in measurement due to bending of the sensor. To ensure that the installation has not affected the FBG properties, the spectral data before and after installation are also compared. Figure 4 shows that the Bragg

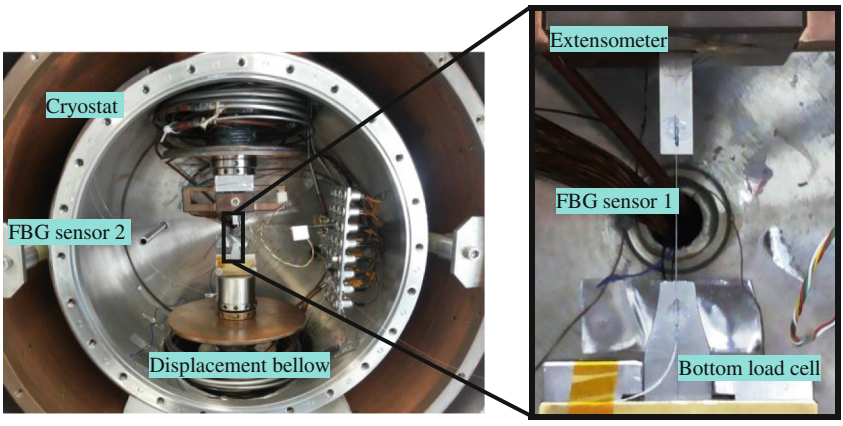

Fig. 6. The sample loaded in the calibration device MTS 25 in a cryostat (left) and the FBG sensor attached to the metal structures is zoomed in for a clear view.

wavelength of the sensor is almost equal before the installation (same as post-heat treatment) and after the installation of the sensor between the load cells.

Keeping the top load cell (extensometer) fixed, the bottom load cell is moved by the displacement bellow (works on hydraulic mechanism) under it for the given displacement values in the command. The given displacement is completely transferred to the FBG sensor, i.e., the change in length of the sensor is equal to the displacement. This induces a strain in the FBG sensor (FBG 1), which in turn causes a Bragg wavelength shift in it. Any temperature changes around it also adds to its Bragg shift ($\Delta\lambda_{B1}$). On the other hand, the Bragg wavelength shift of FBG 2 ($\Delta\lambda_{B2}$) which hangs freely in the cryostat is caused only due to the temperature changes.

After each displacement command it is necessary to wait for about five minutes for the bellow to settle down to the desired displacement. The calibration tests are first performed at room temperature for both straining (downward displacement of bottom load cell) and de-straining (upward movement of bottom load cell). The respective readings of the extensometer, FBG sensor and the displacement bellow are recorded for each given displacement. The test is performed 3 times to check the repeatability of the sensor.

For calibration tests at the desired cryogenic temperature (77 K), the test chamber (cryostat) is cooled down by the attached Liquid Nitrogen (LN_2) pipe up to 100 K. The temperature inside the chamber is monitored using a Si diode (Omega Inc., CYD 208 thermometer). To further cool the cryostat down to 77 K, compressed Helium (He) flow is started inside the pipe attached to the Cu-heat exchanger in the cryostat. Once the temperature reaches 77 K, the He flow is reduced to maintain the temperature constant.

As there are a lot of sources of heat transfer in the cryostat, the temperature might increase if He flow is stopped. Hence, it is important to make sure He flow is continuously regulated to maintain a constant temperature of 77 K. The pressure in the cryostat is maintained at 10^{-4} mbar during the cooling down process. The calibration procedure used at 298 K is repeated for measurements at 77 K. The values of Bragg wavelength shift, displacement, extensometer voltage and temperature are recorded for each given displacement for both room temperature and 77 K.

3 Results and Discussion

For the given displacement values, the response observed from extensometer and FBG sensors are depicted in Fig. 7. It can be seen that the response ($\Delta\lambda_{B1}$) of the strain sensor (FBG 1) has same pattern as that of the displacement. The probe is started at time = 500 s and the displacement is increased (straining) in steps of 4 μm up to 16 μm, with each step being held constant for 5 min. The sensor is then de-strained by decreasing the displacement in the steps of 4 μm back to 0 μm. Hysteresis of both tensile machine and FBG sensor response is evident from the plot as the de-straining phase does not show the same response as straining phase. Towards the end of de-straining a vast difference is seen in the pattern between displacement and Bragg shift. This is due to the hysteresis effect of the tensile machine which has gone below the initial displacement value, but the fiber cannot go below its initial Bragg shift value

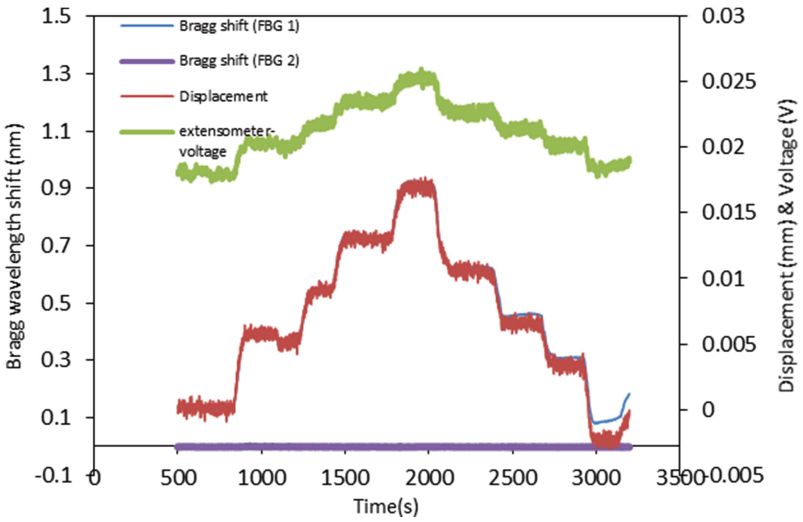

Fig. 7. Response of extensometer and Bragg wavelength for given displacement values.

as it gets completely de-strained at this stage. The figure also shows that the temperature remains constant as the Bragg wavelength shift ($\Delta\lambda_{B2}$) of FBG 2 is constant near zero.

As the given displacement is completely transferred to the sensor, the change in length of the sensor (ΔL) is equal to the given displacement. For each given displacement, the corresponding mechanical strain is calculated based on the attached length of the fiber (L) using the following expression:

$$\varepsilon = \frac{\Delta L}{L} \tag{4}$$

The initial length of the sensor and the corresponding initial Bragg wavelength ($\lambda_{B1,0}$) are taken after providing the sensor with some pre-strain, to ensure that there is no error in the length due to bending of the sensor. The purely strain-dependent Bragg wavelength shift ($\Delta\lambda_B$) is given by the difference of Bragg shift of FBG 1 and FBG 2 as follows:

$$\Delta\lambda_B = |\Delta\lambda_{B1} - \Delta\lambda_{B2}| \tag{5}$$

This Bragg wavelength shift is taken on the y-axis and the induced strain calculated from Eq. 4 is taken on the x-axis as shown Fig. 8. The repeatability test shows that the Bragg wavelength shifts of all the three runs are in good agreement with each other. It can also be observed that the FBG sensor has good repeatability irrespective of the temperature, i.e., the shifts agree with each other for both 298 K and 77 K.

Arithmetic average of the three runs are considered for the calibration plots for both the temperatures. Figure 9 shows the plot of Bragg wavelength shift versus induced strain. It can be observed that the plot is almost linear with little hysteresis effect, i.e.,

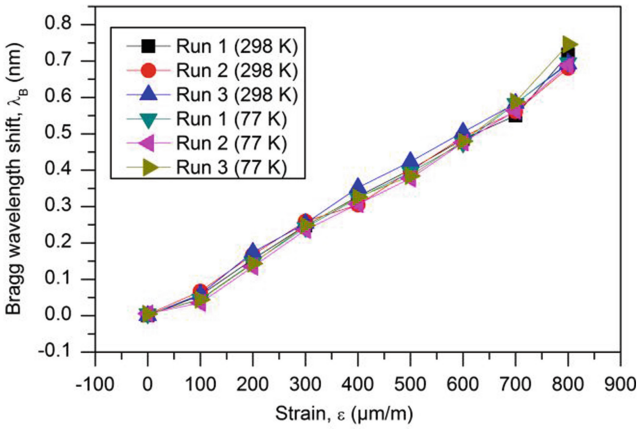

Fig. 8. Repeatability test of FBG strain sensor.

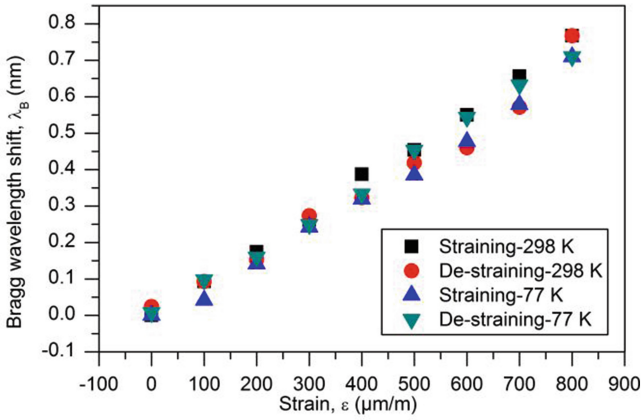

Fig. 9. Bragg wavelength shift (nm) of FBG corresponding to induced strain values at 298 K and 77 K. The legends "Straining" and "De-straining" refer to the measurements performed during straining and de-straining respectively.

for the same induced strain, the wavelength shifts during straining and de-straining phases are slightly different. This is expected out of any experiment and does not affect the calibration much. The hysteresis plots are showed in detail in Fig. 10.

Taking the average of straining and de-straining wavelength shifts for the corresponding strain values, a linear polynomial regression is performed as shown in Fig. 11. It can be observed that the Bragg wavelength shift as a function of induced strain is the same ($\Delta\lambda_B = 0.0009\varepsilon$) for both the cases of temperature with slightly different regression coefficient. In other words, the strain sensitivity of the FBG sensor is found to be 0.9 pm/με at both 298 K and 77 K. Although the linearly regressed equations are the same, there is a visible difference in the individual wavelength shifts. This error could be due to a mild change in glue properties between these temperatures.

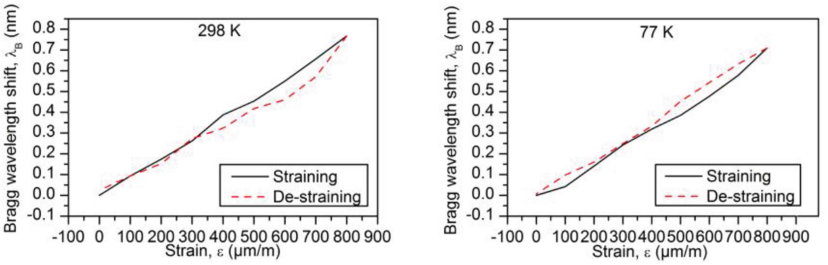

Fig. 10. Hysteresis plots of FBG sensor at 298 K and 77 K. The legends "Straining" and "De-straining" refer to the measurements performed during straining and de-straining of the sensor respectively.

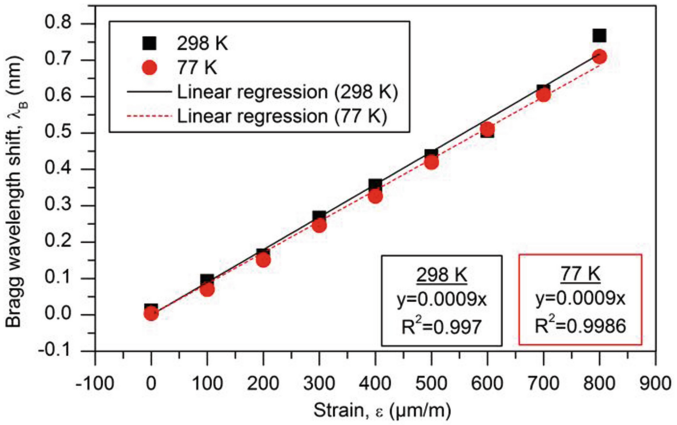

Fig. 11. Calibration measurements of Bragg wavelength shift for corresponding induced strain values at 298 K and 77 K. Linear polynomial regression is described for both the conditions and represented by a solid line for 298 K and dashed line for 77 K. The regression equations for Bragg wavelength shift (y in the graph) as a function of induced strain (x in the graph) are displayed.

The standard deviation between the obtained values and the regressed values is depicted in Fig. 12 in the form of error bars for both the temperatures. The FBG sensor shows less error at 77 K than at 298 K. This can be attributed to the material properties of the optical fiber. It is expected to be more rigid at cryogenic temperatures, hence there will be negligible vibrations in the sensor, which in turn reduces the error in measurements.

As the errors obtained are negligible, the linear equation obtained by regression can be reliably used for this particular sensor. The unknown strain values can be calculated for the observed Bragg wavelength shift and thus, the strain related measurands can be estimated.

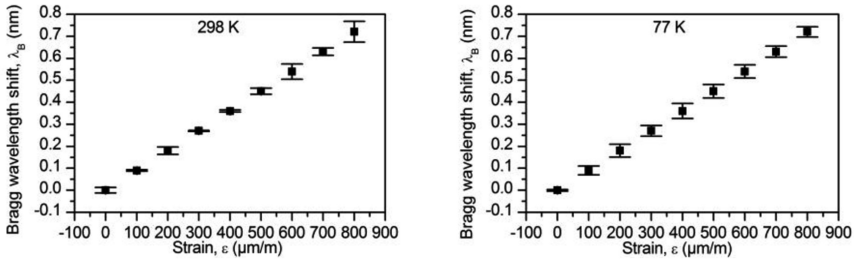

Fig. 12. Error plots of FBG strain sensor between fitted and obtained values of Bragg shift at 298 K and 77 K

4 Conclusions

An effective strain calibration method is implemented for an FBG sensor at room temperature (298 K) and Nitrogen's atmospheric boiling point (77 K). This is a unique and reliable method because the sensing part of the FBG sensor is not attached to any structure or surface. The strain sensitivity of a free, acrylate coated standard FBG sensor is found to be equal (0.9 pm/με) for both the temperatures. A couple of conclusions can be drawn based on the results obtained. As reported in earlier works [14], the strain sensitivity of the FBG sensor did not depend on the temperature. The obtained results also show that the error in measurement is much less at the cryogenic temperature when compared to room temperature. It can be concluded that this method of strain calibration of substrate-free FBG sensor is an effective method that can be used for FBG standardization procedures. Further investigations of strain response will be performed at lower cryogenic temperatures of 10 K and 4 K and analyzed with the results obtained at 298 K and 77 K.

References

1. Rao, Y.J.: Recent progress in applications of in-fibre Bragg grating sensors. Opt. Lasers Eng. **31**(4), 297–324 (1999)
2. Othonos, A., Kalli, K.: Fiber Bragg Gratings – Fundamentals and Application in Telecommunications and Sensing. Artech House Optoelectronics Library, Boston (1999)
3. Iniewski, K.: Smart Sensors for Industrial Applications. Taylor & Francis Group, Boca Raton (2013)
4. Wu, M.-C.: Simultaneous temperature and strain sensing for cryogenic applications using dual-wavelength fiber Bragg gratings. In: Proceedings of SPIE 5191, pp. 208–213 (2003)
5. Ramalingam, R.: Fiber Bragg grating sensors for localized strain measurements at low temperature and in high magnetic field. In: Proceedings of AIP Conference, vol. 1218, no. 1, pp. 1197–1204 (2010)
6. Ramalingam, R., Neumann, H.: Fiber Bragg grating-based temperature distribution evaluation of multilayer insulations between 300 K–77 K. IEEE Sens. J. **11**(4), 1095–1100 (2011)

7. Ramalingam, R., Kläser, M., Schneider, T., Neumann, H.: Fiber Bragg grating sensors for strain measurement at multiple points in an NbTi superconducting sample coil. IEEE Sens. J. **14**(3), 873–881 (2014)
8. Bharathwaj, V., Markan, A., Atrey, M., Neumann, H., Ramalingam, R.: Fiber Bragg gratings for distributed cryogenic temperature measurement in a tube in tube helically coiled heat exchanger. In: IEEE sensors 2014, Valencia, Spain, pp. 1535–1538 (2014)
9. Ramalingam, R., Nast, R., Neumann, H.: Fiber Bragg grating sensors for distributed torsional strain measurements in a (RE) BCO tape. IEEE Sens. J. **15**(4), 2023–2030 (2015)
10. Li, J., Neumann, H., Ramalingam, R.: Design, fabrication, and testing of fiber Bragg grating sensors for cryogenic long-range displacement measurement. Cryogenics **68**, 36–43 (2015). ISSN 0011-2275
11. Kashyap, R.: Fiber Bragg Gratings. Academic Press, San Diego (1999)
12. Othonos, A.: Fiber Bragg gratings. Rev. Sci. Instrum. **68**, 4309–4341 (1997)
13. Roths, J., Andrejevic, G., Kuttler, R., Süsser, M.: Calibration of fiber Bragg cryogenic temperature sensors. In: 18th International Optical Fiber Sensors Conference. Optical Society of America (2006)
14. James, S.W., Tatam, R.P., Twin, A., Morgan, M., Noonan, P.: Strain response of fibre Bragg grating sensors at cryogenic temperatures. Measur. Sci. Technol. **13**, 1535–1539 (2002)
15. Roths, J., Jülich, F.: Determination of strain sensitivity of free fiber Bragg gratings. In: Proceedings of SPIE 7003, p. 700308 (2008)
16. Bagrets, N., Weiss, E., Westenfelder, S., Weiss, K.-P.: Cryogenic test facility CryoMaK. IEEE Trans. Appl. Supercond. **22**(3), 9501204 (2012)
17. Nyilas, A.: Strain sensing systems tailored for tensile measurement of fragile wires. Supercond. Sci. Technol. **18**, S409–S415 (2005)
18. Nyilas, A.: Transducers for sub-micron displacement measurements at cryogenic temperatures. In: Advances in Cryogenic Engineering: Transactions of the Cryogenic Materials Conference – ICMC, vol. 52 (2006)
19. FS22 – Industrial BraggMETER SI. http://www.fibersensing.com/download/0b49e3852b6452701f87b4a06fa4a90d439de5b1